



Communication

Colorimetric recognition of melamine in milk using novel pincer zinc complex stabilized gold nanoparticles

Xiaoling Bao^{a,*,1}, Jianhong Liu^{b,1}, Qingshu Zheng^b, Lixin Duan^b, Yuzhu Zhang^a, Junlong Qian^a, Tao Tu^{b,c,d,*}^a Institute of Quality Inspection of Food and Cosmetics, Shanghai Institute of Quality Inspection and Technical Research, Shanghai 200233, China^b Shanghai Key Laboratory of Molecular Catalysis and Innovative Materials, Department of Chemistry, Fudan University, Shanghai 200438, China^c State Key Laboratory of Organometallic Chemistry, Shanghai Institute of Organic Chemistry, Chinese Academy of Sciences, Shanghai 200032, China^d College of Chemistry and Molecular Engineering, Zhengzhou University, Zhengzhou 450001, China

ARTICLE INFO

Article history:

Received 25 March 2021

Received in revised form 4 April 2021

Accepted 8 April 2021

Available online 10 April 2021

Keywords:

Colorimetric recognition

Gold nanoparticles

Hydrogen-bonding interactions

Pincer zinc complex

Melamine

ABSTRACT

A convenient colorimetric approach for visual detection of melamine in raw milk was realized by using gold nanoparticles (AuNPs) stabilized by an unsymmetrical terpyridyl zinc complex with a thymine fragment at one terminal and a quaternary ammonium salt at the other. Even without pre-addition of melamine or relative additives, obvious color change from red to blue was observed by naked eye in the presence of trace amount of melamine, which was attributed to the alternation of aggregation state of AuNPs caused by the selective binding between the thymine fragment and melamine via triple hydrogen-bonding interactions. Remarkably, the detection limit for melamine was as low as 2.4 ppb, providing a highly sensitive and efficient approach for the visual detection of melamine.

© 2021 Chinese Chemical Society and Institute of Materia Medica, Chinese Academy of Medical Sciences.

Published by Elsevier B.V. All rights reserved.

Melamine has been illegally added to dairy products to increase the “claimed” protein content due to its high nitrogen level (66% by mass) and low price [1–3]. However, ingestion of melamine above the safety limit (1 ppm for infant formula in China) can result in renal failure and even death [4–6], especially for infants [7]. Therefore, it is of great significance to develop simple and highly sensitive methods to detect melamine, especially in dairy samples [8,9]. However, current analytical techniques, such as high-performance liquid chromatography (HPLC) [10], liquid chromatography/mass spectrometry (LC/MS) [11], gas chromatography/mass spectrometry (GC/MS) [12], capillary zone electrophoresis/mass spectrometry (CE/MS) [13], surface-enhanced Raman scattering (SERS) [14], and enzyme-linked immunosorbent assay (ELISA) [15], all require expensive, complicated and heavy instruments within the specialized laboratories, making on-site and real-time melamine detection really difficult and inconvenient [16,17].

Currently, colorimetric recognition based on gold nanoparticles (Au NPs) have drawn increasing attention due to their simple

preparation [18–20], easy functionalization, and visualized read-outs by the naked eye with tailorable optical properties, in which the absorption bands can be adjusted by various external stimulations [21,22]. As molecular recognition events can be easily transformed into color changes (from red to blue) [23–25], which caused by the aggregation of the AuNPs, the AuNPs-based colorimetric assays have been used in melamine sensing [26–29]. Lu *et al.* have developed a MTT-stabilized (MTT = 1-(2-mercaptoethyl)-1,3,5-triazinane-2,4,6-trione) AuNPs-based colorimetric sensor for visual detection of melamine via the triple hydrogen-bonding recognition between melamine and MTT, which resulted in excellent selectivity for detecting melamine in milk and a detection limit as low as ppb level [30]. However, to achieve such low detection limit, 1 μmol/L melamine had to be added in advance to obtain the optimized sensor, which obviously increased the complexity of the detection system.

Recently we have realized the visual recognition of melamine in raw milk without any tedious pretreatment via selective metallo-hydrogel formation base on an unsymmetrical terpyridyl zinc complex with a thymine fragment on one end and a quaternary ammonium salt on the other [31]. Based on this work, here we prepared the AuNPs stabilized by pincer zinc complex (Zn-AuNPs) by attaching the quaternary ammonium terminal of the unsymmetrical terpyridyl zinc complex to gold nanoparticles (AuNPs). The obtained Zn-AuNPs could recognize melamine via colorimetric

* Corresponding author at: Shanghai Key Laboratory of Molecular Catalysis and Innovative Materials, Department of Chemistry, Fudan University, Shanghai 200438, China.

** Corresponding author.

E-mail addresses: baoxl@sqi.org.cn (X. Bao), taotu@fudan.edu.cn (T. Tu).

¹ These authors contributed equally to this work.

change based on the triple hydrogen bonding between melamine and thymine (Fig. 1). The bulkiness of terpyridyl zinc complexes could reduce the number of recognition sites on Au NPs, and thus endow Zn-AuNPs with excellent sensitivity (2.4 ppb) and selectivity to melamine in milk without any additional pre-treatment to the sensor in advance.

The unsymmetrical pincer zinc complex **1** with one thymine and one quaternary ammonium salt at the ends was synthesized via a modified method according to our previous report (Scheme S1 in Supporting information) [31]. The thymine fragment was designed to interact with melamine via hydrogen bonding, while the ammonium tail was introduced to anchor on the surface of Au NPs [32] as well as to increase the solubility of the obtained Zn-AuNPs in water.

AuNPs (~12 nm) were prepared according to literature, which were stabilized by citrate in the aqueous solution [33]. By mixing the citrate-stabilized AuNPs aqueous solution with the pincer zinc complex, the desired Zn-AuNPs were obtained via ligand-exchange. The zeta potentials for AuNPs (−35.9 mV) shifted to −26.5 mV after being modified with the pincer zinc complex **1** (Fig. S2 in Supporting information), confirming that the pincer zinc complex was successfully attached to the gold surface [32]. These Zn-AuNPs could be well dispersed in distilled water to form homogenous sensor solution, which showed a color of wine red (Fig. 2a) originated from the strong surface plasmon resonance (SPR) of Au NPs at 525 nm. After adding melamine to Zn-AuNPs, the nanoparticles were aggregated together, inducing an obvious color change from red to blue (insets in Fig. 2). TEM images further confirmed that Zn-AuNPs was highly dispersed in the absence of melamine, and significant aggregation was observed in the presence of 1.2 μmol/L melamine. The aggregation was further supported by the dynamic light scattering (DLS) results (Fig. S3 in Supporting information), in which the particle sizes increased with the increase of melamine amount (0.2, 0.35 and 0.5 μmol/L), and the size distribution also become broader.

To confirm the presence of triple hydrogen-bonding interactions, we performed a series of investigations. ¹H NMR spectra of the unsymmetrical pincer zinc complex **1** with different amount of melamine were measured in DMSO-*d*₆ and CDCl₃-*d* (V_{DMSO}:V_{CDCl₃} = 1:1). DMSO had to be incorporated as a co-solvent due to the poor solubility of melamine in chloroform. As can be seen in Fig. S4 (Supporting information), the chemical shift of N—H proton (H_a) of the imidodicarbonyl group in **1** shifted from 11.12 ppm to 11.35 ppm. The obvious downfield shift implied that the secondary amine of **1** was markedly influenced by hydrogen-bonding interactions between the hydrogen protons (H_b) of imide group and nitrogen atoms of the triazine ring. In addition, the

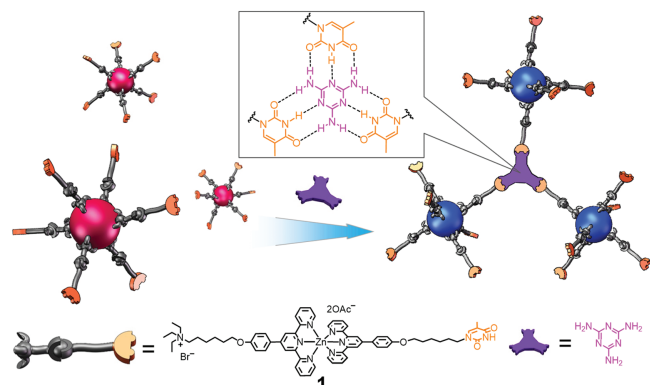


Fig. 1. Colorimetric recognition of melamine using the terpyridyl zinc complex-stabilized gold nanoparticles (Zn-AuNPs) via hydrogen-bonding between melamine and thymine moiety.

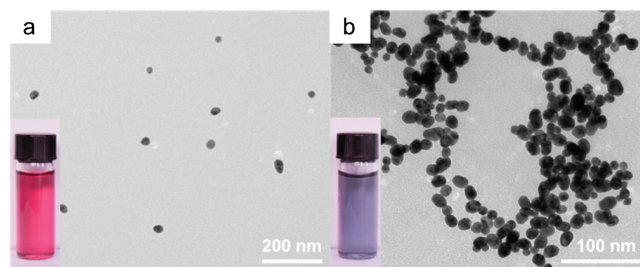


Fig. 2. TEM images and the corresponding images under ambient light (insets) of the terpyridyl zinc complex-stabilized gold nanoparticles (a) without and (b) with the presence of melamine (1.2 μmol/L).

chemical shift of N—H proton (H_a) of melamine shifted from 5.79 ppm to 5.74 ppm in ¹H NMR spectrum further confirmed the triple hydrogen-bonding interactions between thymine fragment and melamine. The formation of intermolecular hydrogen bonds was also characterized by Fourier transform infrared (FT-IR) spectroscopy. As shown in Fig. S5 (Supporting information), three principal absorption regions (3000–3500, 1400–1700 and 800–1050 cm^{−1}) were observed in the FT-IR spectrum of melamine [34]. The 3000–3500 cm^{−1} region encompassed the N—H stretching modes, and the two sharp high frequency bands (3468 and 3419 cm^{−1}) shifted to 3193 cm^{−1}. The apparent red-shift confirmed the formation of hydrogen bonds between N—H (H_a) protons of melamine and C=O group of the imidodicarbonyl functional group [35].

Further quantitative recognition analysis was studied by adding different amounts of melamine to an aqueous solution of the Zn-AuNPs (2.0 nmol/L). With the addition of melamine (0–0.5 μmol/L), the color of the Zn-AuNPs solution changed from wine red to blue (Fig. 3a). In UV–vis spectra, the absorption band at 525 nm, which corresponded to dispersed Zn-AuNPs [30], decreased along with the increase of melamine amount, whereas the intensity of the signal at 663 nm corresponding to gathered Zn-AuNPs showed an inverse increasing trend (Fig. 3b) [33]. In other words, upon adding more melamine, the Zn-AuNPs solution absorbed less green light but more red light, thus inducing a visible color change from red to blue (Fig. 3a). This observation was ascribed to the assembly between melamine and thymine moiety of the zinc complex via the complementary triple hydrogen-bonding interactions.

To gain a better understanding of the colorimetric change, the intensity ratio $A_{663 \text{ nm}}/A_{525 \text{ nm}}$ of Zn-AuNP solution was employed to

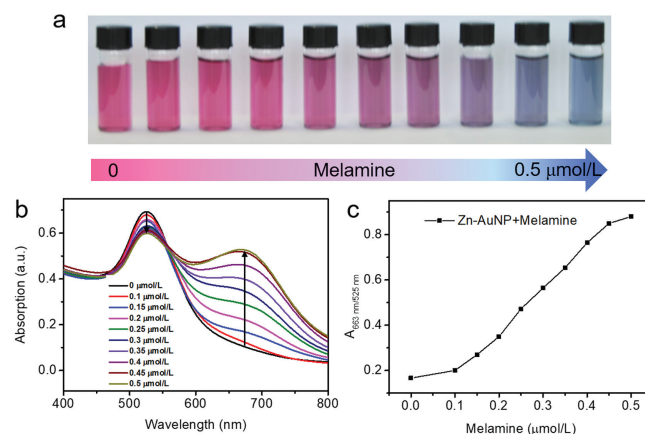


Fig. 3. (a) The photographs of the Zn-AuNPs generated in the presence of different concentrations of melamine (0–0.5 μmol/L). (b) The corresponding UV–vis spectra of the Zn-AuNPs solutions. Spectra were recorded after a fixed time interval of 15 min. (c) Absorbance ratio ($A_{663 \text{ nm}}/A_{525 \text{ nm}}$) of the Zn-AuNPs against melamine concentrations.

give a quantitative description. As shown in Fig. 3c, the value of $A_{663\text{ nm}/525\text{ nm}}$ increased sharply from ~ 0.1 to 0.5 along with the increasing concentration of melamine over the range of 0.1–0.5 $\mu\text{mol/L}$. More importantly, a good linear relationship ($R^2 = 0.998$) between $A_{663\text{ nm}/525\text{ nm}}$ and melamine concentration was obtained over the range of 0.1–0.45 $\mu\text{mol/L}$, which means this sensor system could be used as a quantitative determination tool for melamine detection (Fig. S6 in Supporting information). The detection limit (3δ) was calculated to be *ca.* 2.4 ppb (see Supporting information for details). Compared with reported methods based on gold nanoparticles for melamine detection (Table S1 in Supporting information), this method has high sensitivity for quantitative analysis of melamine.

To further probe the role of the triple hydrogen-bonding interactions, the influence of pH was then investigated (Fig. 4b). Zn-AuNP solutions with same concentration (2 nmol/L) but different pH values (5, 7 and 9) were employed for UV-vis tests. The intensity of $A_{663\text{ nm}/525\text{ nm}}$ increased sharply under neutral condition, while minor change or almost the same values were obtained under acidic or basic conditions. These observations were attributed to the protonation and deprotonation of the thymine moiety in acidic and basic media, which interfered the formation of triple hydrogen-bonding between the thymine moieties and melamine.

Under neutral conditions, the value of $A_{663\text{ nm}/525\text{ nm}}$ for the Zn-AuNPs system keep increasing in 10 min upon addition of melamine and then reached saturation within 15 min (Fig. 4a, black squares). As a comparison, the value of $A_{663\text{ nm}/525\text{ nm}}$ for the Zn-AuNPs system without melamine remained below 0.2 (Fig. 4a, red circles). Therefore, for quantitative determination of melamine, the optimal detection time should be over 15 min. For qualitative recognition, the color changes could be observed within a few minutes, providing a rapid and naked-eye-distinguishable color change.

A big challenge for detecting melamine in commercially available milk was how to selectively distinguish melamine and diminish the potential interference from other common ingredients in milk like amino acids, illegal/legal additives including sugars, vitamins and urea. To evaluate the selectivity of Zn-AuNPs towards melamine, control experiments involving the glucose, vitamin B, cyanuric acid, lactose, nucleic acid, glycolic acid, maltose, fructose, ascorbic acid, ammelide, ammeline, and melamine were carried out. As shown in Fig. 5, among all of the test molecules, only melamine caused an obvious increase in the $A_{663\text{ nm}/525\text{ nm}}$ value, indicating that this melamine sensor had high selectivity against these residual ingredients. The specificity of triple hydrogen-bonding between the thymine fragment of Zn-AuNPs and melamine was believed to be responsible for the high selectivity, though all these selected substances can form weak hydrogen bonds with thymine fragment.

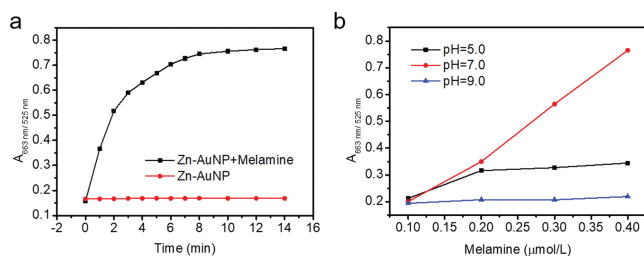


Fig. 4. (a) Effects of response time on the absorbance ratio ($A_{663\text{ nm}/525\text{ nm}}$) of the Zn-AuNPs in the absence and presence of melamine (0.5 $\mu\text{mol/L}$). (b) Effects of pH on the absorbance ratio ($A_{663\text{ nm}/525\text{ nm}}$) of the Zn-AuNPs in the presence of melamine (0.1–0.4 $\mu\text{mol/L}$).

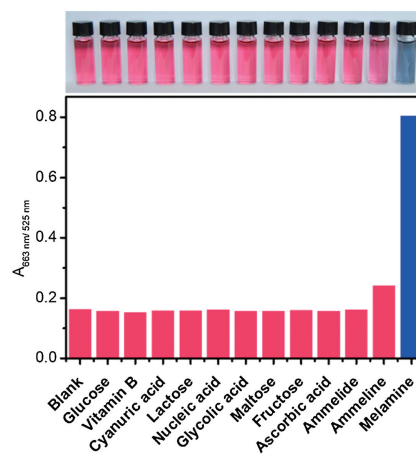


Fig. 5. Images and absorbance ratio ($A_{663\text{ nm}/525\text{ nm}}$) of the Zn-AuNPs toward melamine and different interfering molecules (0.5 $\mu\text{mol/L}$).

Table 1
Determination of melamine content in milk samples.

Samples	Added ($\times 10^{-7}$ mol/L)	Found ($\times 10^{-7}$ mol/L) ^a	Recovery (%) ^a
1	2.0	1.95 ± 0.07	97.5 ± 3.5
2	3.0	3.01 ± 0.04	100.3 ± 1.3
3	4.0	4.06 ± 0.05	101.5 ± 1.2

^a Mean \pm std, n = 5.

Having known the excellent selectivity and sensitivity of the Zn-AuNPs towards melamine over other possible ingredients in milk, such a colorimetric sensor was then employed for detection of melamine in milk. To gain better color sensitivity, the raw milk had to be pretreated through an extraction procedure (Supporting information for details) to remove most proteins and other insoluble ingredients and obtain a colorless clear solution [30]. The concentration of melamine in the samples was measured by the standard addition method and the results are summarized in Table 1. As can be seen, the recoveries of melamine were within the range from 97.5% to 101.5%. Thus, the proposed sensing system is reliable and suitable for real applications.

In conclusion, gold nanoparticles stabilized by an unsymmetrical terpyridyl zinc complex with a thymine fragment at one terminal and a quaternary ammonium salt at the other was synthesized, which could selectively discriminate melamine in milk with obviously colorimetric change from red to blue without any melamine pre-addition and any interference from other milk ingredients. The detection limit of melamine was as low as 2.4 ppb, which was attributed to the specific triple hydrogen-bonding between the thymine fragment and melamine. Compared with current melamine detection techniques, the method does not require expensive and complicated instruments, thus enabling rapid and ultrasensitive detection of melamine in dairy products.

Declaration of competing interest

The authors report no declarations of interest.

Acknowledgments

Financial support from the State General Administration of the People's Republic of China for Quality Supervision and Inspection and Quarantine (No. 2016QK122), the Science and Technology Projects of Jiangxi Province (No. 20181BBH80007), Shanghai Institute of Quality Inspection and Technical Research, and the

Department of Chemistry, Fudan University is gratefully acknowledged.

Appendix A. Supplementary data

Supplementary material related to this article can be found, in the online version, at doi:<https://doi.org/10.1016/j.ccllet.2021.04.014>.

References

- [1] H. Zhu, N. Wang, Y. Xu, et al., *Adv. Funct. Mater.* 26 (2016) 3029–3035.
- [2] S. Xu, G. Lin, W. Zhao, et al., *ACS Appl. Mater. Interfaces* 10 (2018) 24850–24859.
- [3] L. Tang, S. Mo, S.G. Liu, et al., *J. Agric. Food Chem.* 66 (2018) 2174–2179.
- [4] Y. Lu, Y. Xia, G. Liu, et al., *Crit. Rev. Anal. Chem.* 47 (2017) 51–66.
- [5] S. Pan, D. Yao, A. Liang, et al., *ACS Appl. Mater. Interfaces* 12 (2020) 12120–12132.
- [6] M. Shellaiah, K.W. Sun, *Chemosensors* 7 (2019) 9.
- [7] M. Farrokhnia, S. Karimi, S. Askarian, *ACS Sustain. Chem. Eng.* 7 (2019) 6672–6684.
- [8] M.B. Regasa, T.R. Soreta, O.E. Femi, et al., *ACS Omega* 5 (2020) 4090–4099.
- [9] X. Han, Z. Qin, M. Zhao, et al., *RSC Adv.* 8 (2018) 34877–34882.
- [10] W. Fan, M. Gao, M. He, et al., *Analyst* 140 (2015) 4057–4067.
- [11] J. Draher, S. Ehling, N. Cellar, et al., *Rapid Commun. Mass Spectrom.* 30 (2016) 1265–1272.
- [12] Y.L. Wong, C. Mok, *Anal. Methods* 5 (2013) 2305–2314.
- [13] M. Himmelsbach, T.D.T. Vo, *Electrophoresis* 35 (2014) 1362–1367.
- [14] X. Liang, X. Zhang, T. You, et al., *J. Raman Spectrosc.* 49 (2018) 245–255.
- [15] W. Yin, J. Liu, T. Zhang, et al., *J. Agric. Food Chem.* 58 (2010) 8152–8157.
- [16] G. Zhang, Y. Chen, J. Xie, et al., *RSC Adv.* 9 (2019) 36266–36270.
- [17] I.E. Paul, A. Rajeshwari, T.C. Prathna, et al., *Anal. Methods* 7 (2015) 1453–1462.
- [18] F. Wang, Y. Lu, Y. Chen, et al., *ACS Sustain. Chem. Eng.* 6 (2018) 3706–3713.
- [19] M. Shi, Z. Wang, *Chem. Asian J.* 15 (2020) 1–10.
- [20] L. Yu, N. Li, *Chemosensors* 7 (2019) 53.
- [21] C. Yuan, J. Jiang, D. Wang, et al., *J. Nanosci. Nanotechnol.* 19 (2019) 2789–2793.
- [22] D. Yang, P. Liu, W. Lin, et al., *Chem. Asian J.* 15 (2020) 2499–2504.
- [23] G. Liu, M. Lu, X. Huang, et al., *Sensors* 18 (2018) 4166.
- [24] S. Su, J. Li, Y. Yao, et al., *ACS Appl. Bio Mater.* 2 (2019) 292–298.
- [25] P.A. Mirau, J.E. Smith, J.L. Chávez, et al., *Langmuir* 34 (2018) 2139–2146.
- [26] J. Zhao, H. Wu, J. Jiang, et al., *RSC Adv.* 4 (2014) 61667–61672.
- [27] X. Liu, F. He, F. Zhang, et al., *Anal. Chem.* 92 (2020) 9370–9378.
- [28] L. Chen, Y. Huang, T.T. Xing, et al., *J. Mater. Chem. C* 5 (2017) 7806–7812.
- [29] J. Liu, S. Feng, Y. Shi, et al., *Anal. Methods* 7 (2015) 5162–5168.
- [30] K. Ai, Y. Liu, L. Lu, *J. Am. Chem. Soc.* 131 (2009) 9496–9497.
- [31] X. Bao, J. Liu, Q. Zheng, et al., *Chin. Chem. Lett.* 30 (2019) 2266–2270.
- [32] J. Du, Z. Wang, X. Peng, et al., *Ind. Eng. Chem. Res.* 54 (2015) 12011–12016.
- [33] C. Xiao, X. Zhang, J. Liu, et al., *Anal. Methods* 7 (2015) 924–929.
- [34] L. Li, G. Wu, T. Hong, et al., *ACS Appl. Mater. Interfaces* 6 (2014) 2858–2864.
- [35] Z. Nie, B. Zuo, L. Liu, et al., *Macromolecules* 53 (2020) 4204–4213.